

Chapter 5

Topological insulators and superconductors

Learning goals

- We know the Kane Mele model.
 - We can derive the topological index based on time reversal polarization.
 - We understand the entries of the periodic table for topological insulators.
 - We know what a $p_x + ip_y$ superconductor is.
 - We are acquainted with the Kitaev wire.
 - We know the Su-Schrieffer-Heeger model.
-
- M. König et al., Science **318**, 766 (2007)

In this chapter we try to understand what topological properties can arise for free fermion systems subject to some symmetry constraints. The exposition starts from a historical perspective with the first time-reversal symmetric topological insulator in two dimensions by Kane and Mele [1]. We then motivate on physical grounds how one can construct a topological index characterizing this new type of band insulator. Our derivation follows the historically motivated path covered in the book by Bernevig and Hughes [2]. The so derived topological index for two-dimensional systems readily generalizes to three dimensions. Once we established the presence of two- and three-dimensional topological insulators protected by time-reversal symmetry we take a somewhat more formal perspective and discuss the *periodic table for topological insulators* which catalogues all symmetry protected topological free fermion systems. We learn how to read and use the table and relate its entries to experimentally relevant response functions. Finally, we conclude this chapter by covering three archetypal models in different symmetry classes.

5.1 The Kane-Mele model

In the last chapter we have seen that we can construct lattice models where the Bloch bands have a non-vanishing Chern number despite the absence of a net magnetic field. Here we try to build a time-reversal invariant version based on Haldane's honeycomb model for a Chern insulator.

We start from the low energy version of graphene

$$H_0 = -i\hbar v_F [\sigma_x \tau_z \partial_x + \sigma_y \partial_y], \quad (5.1)$$

where σ acts on the sub-lattice index and τ on the valley (K, K') space.

Let us add spin s to the game. With this we arrive at an 8×8 problem. The question is what kind of terms can we add in order to open a “non-trivial” gap. We have seen that

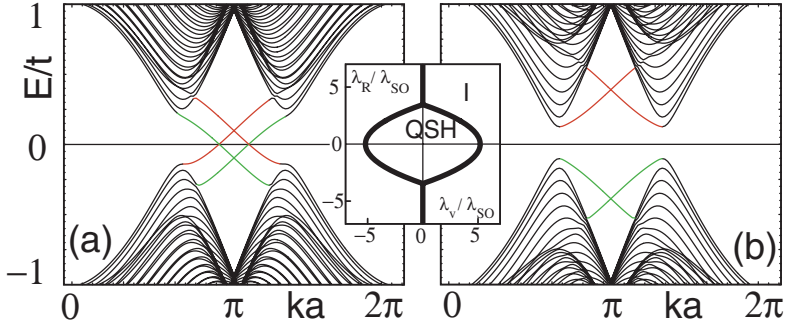


Figure 5.1: Edge spectrum of the Kane Mele model for two different values of λ_R . On the left, two edge states cross the gap (colors label the edge). On the right, no edge states cross the gap. The inset shows the phase diagram as a function of λ_v and λ_R . Figure taken from Ref. [1] (Copyright (2005) by The American Physical Society).

$m\sigma_z + \tau_z\sigma_z 3\sqrt{3}t \sin(\varphi)$ does the job. However, this is not time-reversal symmetric for $\varphi \neq 0, \pi$ and m alone opens trivial gaps with $\mathcal{C} = 0$.

We construct a “non-trivial” time-reversal invariant gap step by step. First, in the sub-lattice space we need a σ_z term, otherwise we just move around the K and K' Dirac points in \mathbf{k} -space. Next, we need a spin dependent (\mathbf{s}) part to couple the two copies of the Haldane model. Let us try for the K point

$$\sigma_z \otimes s_z = \begin{pmatrix} \sigma_z & 0 \\ 0 & -\sigma_z \end{pmatrix}, \quad (5.2)$$

which gives us different gaps [with different “sign(m)”] for the two spins. How do we now add the valley degree of freedom ($\boldsymbol{\tau}$) in order to make it time-reversal invariant? The \mathcal{T} -operator acts in sub-lattice and spin space as

$$\mathcal{T} = \mathbb{1}_\sigma \otimes i s_y K = \begin{pmatrix} 0 & -\mathbb{1}_\sigma \\ \mathbb{1}_\sigma & 0 \end{pmatrix}. \quad (5.3)$$

Therefore, the term $\propto \sigma_z \otimes s_z$ transforms as

$$\begin{aligned} \mathcal{T} \sigma_z \otimes s_z \mathcal{T}^{-1} &= \begin{pmatrix} 0 & -\mathbb{1}_\sigma \\ \mathbb{1}_\sigma & 0 \end{pmatrix} \begin{pmatrix} \sigma_z & 0 \\ 0 & -\sigma_z \end{pmatrix} \begin{pmatrix} 0 & \mathbb{1}_\sigma \\ -\mathbb{1}_\sigma & 0 \end{pmatrix} \\ &= \begin{pmatrix} 0 & -\mathbb{1}_\sigma \\ \mathbb{1}_\sigma & 0 \end{pmatrix} \begin{pmatrix} 0 & \sigma_z \\ \sigma_z & 0 \end{pmatrix} = \begin{pmatrix} -\sigma_z & 0 \\ 0 & \sigma_z \end{pmatrix} = -\sigma_z \otimes s_z. \end{aligned} \quad (5.4)$$

Under time reversal, $K \rightarrow K'$. Hence, we need the gap opening term in K' to be $\mathcal{T} \sigma_z \otimes s_z \mathcal{T}^{-1} = -\sigma_z \otimes s_z$ to have $\mathcal{T} H(\mathbf{k}) \mathcal{T}^{-1} = H(-\mathbf{k})$. From this we conclude that the full gap opening term should be of the form

$$H_{\text{KM}} = \lambda_{\text{SO}} \sigma_z \otimes \tau_z \otimes s_z. \quad (5.5)$$

We labelled the interaction with spin-orbit (λ_{SO}) to stress that H_{KM} couples spin (s_z) and orbital (τ_z) degrees of freedom. Moreover, H_{KM} is time-reversal invariant (TRI) by construction. Reverse engineering to a full lattice model we find

$$H_{\text{KM}} = \sum_{\langle i,j \rangle, \alpha} c_{i\alpha}^\dagger c_{j\alpha} + i \lambda_{\text{SO}} \sum_{\langle\langle i,j \rangle\rangle, \alpha\beta} \nu_{ij} c_{i\alpha}^\dagger s_{\alpha\beta}^z c_{j\beta} + \lambda_v \sum_{i\alpha} \epsilon_i c_{i,\alpha}^\dagger c_{i,\alpha}, \quad (5.6)$$

where ϵ_i and the sign strucutre of ν_{ij} are the same as in Haldane’s ’88 model [3]. The above model was the first TRI topological insulator proposed by Kane and Mele in 2005 [1]. As

it is TRI, the total Chern number cannot be non-zero. However, in the form (5.6), the spin projections $|\uparrow\rangle$, $|\downarrow\rangle$ are good eigenstates. Therefore, we can use the Chern number \mathcal{C}_σ in each spin-sector to characterize the phases. Indeed

$$\nu = \frac{C_\uparrow - C_\downarrow}{2} \bmod 2 \in \mathbb{Z}_2 \quad (5.7)$$

defines a good topological index as we will see below [4]. The addition of a Rashba term

$$H_R = \lambda_R [\sigma_x \tau_z s_x - \sigma_y s_x] \quad (5.8)$$

removes this conserved quantity. While H_R does not open a gap by itself (why?), it can influence the λ_{SO} induced gap, see Fig. 5.1. However, the above topological index ν is not well defined anymore. In the following section we aim at deriving a \mathbb{Z}_2 index which does not rely on spin-Chern numbers.

5.2 \mathbb{Z}_2 index

5.2.1 Charge polarization

We revisit Laughlin's pumping argument to make progress towards a \mathbb{Z}_2 index for TRI topological insulators. We consider a one dimensional system on a lattice (with lattice constant $a = 1$) with Bloch wave functions

$$|\psi_{n,k}\rangle = \frac{1}{\sqrt{L}} e^{ikx} |\varphi_{nk}(x)\rangle \quad \text{with} \quad |\varphi_{nk}(x)\rangle = |\varphi_{nk}(x+1)\rangle. \quad (5.9)$$

The corresponding Wannier functions are defined as

$$|W_{nR}(x)\rangle = \frac{1}{2\pi} \int_{-\pi}^{\pi} dk e^{ik(R-x)} |\varphi_{nk}(x)\rangle, \quad (5.10)$$

with $R = m \in \mathbb{Z}$ a lattice vector. Note that the Wannier functions are not gauge invariant as the relative phase between different $|\varphi_{nk}(x)\rangle$ is not a priori fixed. However, for a filled band, the Slater determinant is insensitive to a unitary transformation (which the transformation to Wannier states is) among the filled states. For a smooth gauge, the Wannier functions are exponentially localized around a well defined center [5].

The total charge polarization is now defined as

$$P = \sum_{n \text{ filled}} \int dx \langle W_{0n}(x) | x | W_{0n}(x) \rangle. \quad (5.11)$$

We try to write this polarization in a more familiar way

$$P = \sum_{n \text{ filled}} \frac{1}{(2\pi)^2} \frac{1}{L} \int_{-\pi}^{\pi} dk_1 \int_{-\pi}^{\pi} dk_2 e^{i(k_1 - k_2)x} \langle \varphi_{nk_1} | i\partial_k | \varphi_{nk_2} \rangle \quad (5.12)$$

$$= \sum_{n \text{ filled}} \frac{i}{2\pi} \int_{-\pi}^{\pi} dk \langle \varphi_{nk} | i\partial_k | \varphi_{nk} \rangle = \frac{1}{2\pi} \int_{-\pi}^{\pi} dk \mathcal{A}_x(k), \quad (5.13)$$

with

$$\mathcal{A}_x(k) = \sum_{n \text{ filled}} i \langle \varphi_{nk} | \partial_k | \varphi_{nk} \rangle. \quad (5.14)$$

Two comments are in order:

1. If we re-gauge $|\varphi\rangle \rightarrow e^{i\vartheta(k)}|\varphi\rangle$ with a $\vartheta(k)$ that is winding by $2\pi m$ throughout the Brillouin zone, the corresponding polarization changes to

$$P \rightarrow P + m.$$

This is ok, as charge polarization is anyway only defined up to a lattice constant.

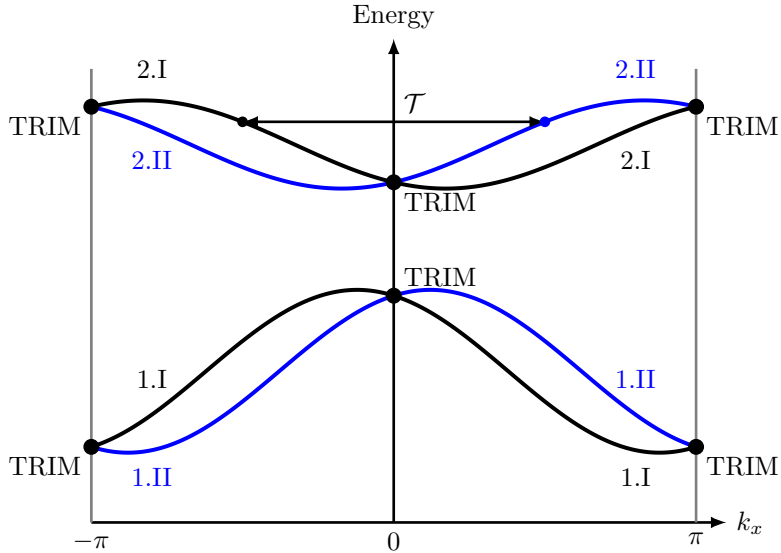


Figure 5.2: Energy levels for a time reversal invariant system.

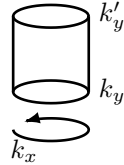
2. P depends on the chosen gauge. But *changes in P by a smooth change in system parameters are gauge independent*. So let us imagine a tuning parameter k_y with

$$H(k_y) \rightarrow H(k'_y)$$

which is slow in time. The change in charge polarization is given by

$$\Delta P = \frac{1}{2\pi} \left[\int_{-\pi}^{\pi} dk \mathcal{A}(k, k_y) - \int_{-\pi}^{\pi} dk \mathcal{A}(k, k'_y) \right] \quad (5.15)$$

If we use Stokes' theorem we arrive at



$$\Delta P = \int_{k_y}^{k'_y} dk_y \int_{-\pi}^{\pi} dk \mathcal{F}(k, k_y). \quad (5.16)$$

By choosing $k'_y = k_y + 2\pi$, we find for the change in charge polarization $\Delta P = \mathcal{C}$ where \mathcal{C} is the Chern number. We know, however, that $\mathcal{C} \sim \sigma_{xy}$ and hence is equal to zero for TRI systems.

Building on the above insight we try to refine the charge pumping of Laughlin to be able to characterize a TRI system.

5.2.2 Time reversal polarization

Let us now try to generalize the charge pumping approach to the TRI setup. For this it is beneficial to look at the structure of a generic energy diagram as shown in Fig 5.2. Under time-reversal, momenta k are mapped to $-k$. Moreover, there are special points in the Brillouin zone which are mapped onto themselves. This is true for all momenta which fulfill $k = -k + G$, where G is a reciprocal lattice vector. This is trivially true for $k = 0$, but also for special points

on the borders of the Brillouin zone. On such time reversal invariant momenta (TRIM's), the spectrum has to be doubly degenerate due to Kramer's theorem.

Owing to the symmetry between k and $-k$ we can constrain ourselves to only *half the Brillouin zone*. In this half, we label all bands by I.I, I.II, 2.I, 2.II, The arabic number simply label pairs of bands. Due to the double degeneracy at the TRIMs, we need an additional (roman number) to label the two (sub)-bands emerging from the TRIMs. One can also say that the roman index labels Kramers pairs

$$\mathcal{T}|\varphi_{n,\text{I}}(k)\rangle = e^{i\chi_{n,k}}|\varphi_{n,\text{II}}(-k)\rangle. \quad (5.17)$$

We now try to construct the polarization for only one of the two labels $s = \text{I}$ or II

$$P^s = \frac{1}{2\pi} \int_{-\pi}^{\pi} dk \mathcal{A}^s(k) \quad \text{with} \quad \mathcal{A}^s(k) = i \sum_{n \text{ filled}} \langle \varphi_{n,s}(k) | \partial_k | \varphi_{n,s}(k) \rangle. \quad (5.18)$$

It is clear that $P = P^{\text{I}} + P^{\text{II}}$ will vanish. However, the same must not hold for the *time reversal polarization*

$$P^{\mathcal{T}} = P^{\text{I}} - P^{\text{II}}. \quad (5.19)$$

The problem is, that we assigned the labels I and II. It is not a priori clear if this can be done in a gauge invariant fashion. In particular, the Slater determinant of a band insulator with $2n$ filled bands has a $SU(2n)$ symmetry, as basis changes of filled states do not affect the total wave function. With our procedure we explicitly broke this $SU(2n)$ symmetry. There is a way however, to formulate the same \mathcal{T} -polarization $P^{\mathcal{T}}$ in a way that does not rely on a specific labeling of the Kramers pairs. This can be achieved by the use of the so-called *sewing matrix* [2]

$$B_{mn}(k) = \langle \varphi_m(-k) | \mathcal{T} | \varphi_n(k) \rangle. \quad (5.20)$$

$B(k)$ has the following properties: (i) it is unitary, and (ii) it is anti-symmetric, i.e., $B^T(k) = -B(k)$ only if k is a TRIM. Using this matrix one can show that

$$P^{\mathcal{T}} = \frac{1}{i\pi} \log \left[\frac{\sqrt{\det B(\pi)}}{\text{Pf } B(\pi)} \frac{\text{Pf } B(0)}{\sqrt{\det B(0)}} \right]. \quad (5.21)$$

This expression is manifestly invariant under $SU(2n)$ rotations within the filled bands. Moreover, it only depends on the two TRIMs $k = 0, \pi$, and it is defined modulo two.

The Pfaffian $\text{Pf } B(k)$ of a $2n \times 2n$ anti-symmetric matrix matrix B is defined as

$$\text{Pf } B = \frac{1}{2^n n!} \sum_{\sigma \in S_{2n}} \text{sign}(\sigma) \prod_{i=1}^n b_{\sigma(2i-1), \sigma(1i)} \quad (5.22)$$

with the property

$$\text{Pf}^2 B = \det B. \quad (5.23)$$

Let us now see how we can describe changes in the time-reversal polarization under the influence of an additional parameter k_y . Written as in (5.21), it is only defined for $k_y = 0, \pi, 2\pi$, i.e, at TRIMs. In Fig. 5.3 we illustrate what we can expect from such a smooth change. We start at $k_y = 0$. If we now change k_y slowly, we know that due to TRI, we cannot build up a charge polarization. However, the Wannier centers of two Kramers pairs will evolve in opposite direction. At $k_y = \pi$, we can check how far these centers evolved away from each other. As $P^{\mathcal{T}}$ is well defined and equal to 0 or 1 we have two options: (i) Each Wannier center meets up with one coming from a neighboring site [Fig. 5.3(a)]. This gives rise to $P^{\mathcal{T}}(k_y = \pi) = 1$ and

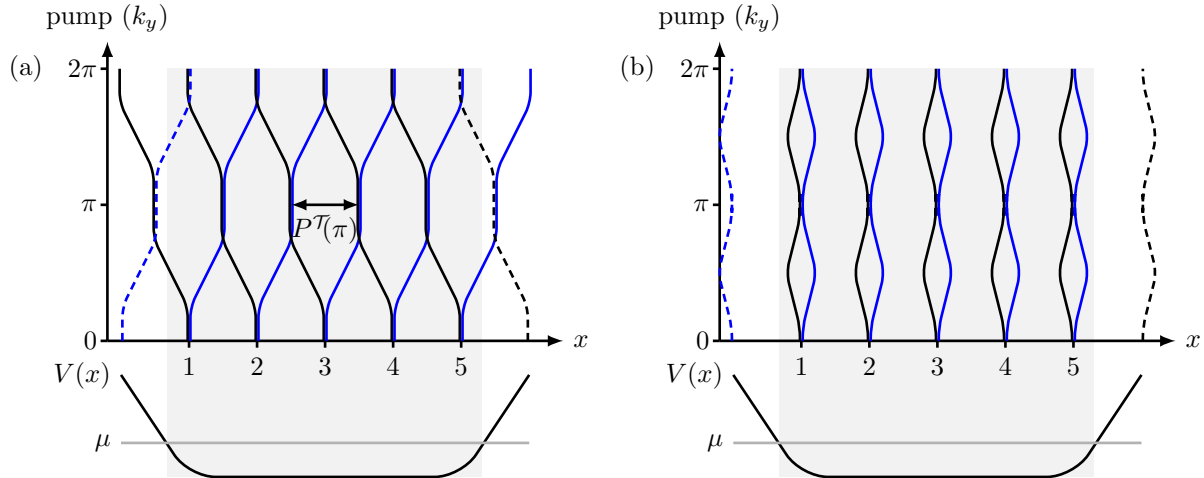


Figure 5.3: (a) Pumping of time reversal polarization in a topologically non-trivial state. (b) Pumping of time reversal polarization in a trivial state.

this effect is called *pair switching*. (ii) The centers fall back onto each other again [Fig. 5.3(b)], resulting in $P^T(k_y = \pi) = 0$.

Let us further assume that we have a smooth confining potential $V(x)$ in x -direction. As in the case of the quantum Hall effect, we see how states can be pushed up-hill or pulled down-hill as a function of k_y . However, as opposed to the quantum Hall effect, we have here the situation that on each edge we have both a state coming down in energy as well as one climbing up! From that we conclude that if we have pair-switching, we expect two counter-propagating edge states on *both sides of the sample*.

We can now construct a topological index for the two-dimensional system: If the \mathcal{T} -polarization at $k_y = 0$ and $k_y = \pi$ differ by one, we expect an odd number of pairs of edge states. Hence, we define

$$\nu = \prod_{l=1}^4 \frac{\sqrt{\det B(\Lambda_l)}}{\text{Pf } B(\Lambda_l)} \in \mathbb{Z}_2 \quad \text{with} \quad \Lambda_l : \text{TRIM}. \quad (5.24)$$

5.2.3 Three dimensional topological insulators

The above formulation immediately suggests a three-dimensional generalization of the \mathbb{Z}_2 index

$$\nu_s = \prod_{l=1}^8 \frac{\sqrt{\det B(\Lambda_l)}}{\text{Pf } B(\Lambda_l)} \in \mathbb{Z}_2 \quad \text{with} \quad \Lambda_l : \text{TRIM}, \quad (5.25)$$

where now the product runs over all eight TRIMs of the three-dimensional Brillouin zone shown in Fig. 5.4. This index is called the *strong* topological index. Additionally, one can think of a three-dimensional system to be made out of planes of two-dimensional topological insulators. In Fig. 5.5 we show how one can attribute a *weak* topological index (ν_x, ν_y, ν_z) corresponding to the stacking directions.

According to our reasoning above, when we cut the system perpendicular to the direction defined by the weak index, we expect *two Dirac cones* on the resulting surface (why?). However, if we have a strong topological index, there is a single Dirac cone irrespective of the way we terminate the bulk system. To wrap up, we mention that one usually gathers the indices to

$$\boldsymbol{\nu} = (\nu_s; \nu_x, \nu_y, \nu_z). \quad (5.26)$$

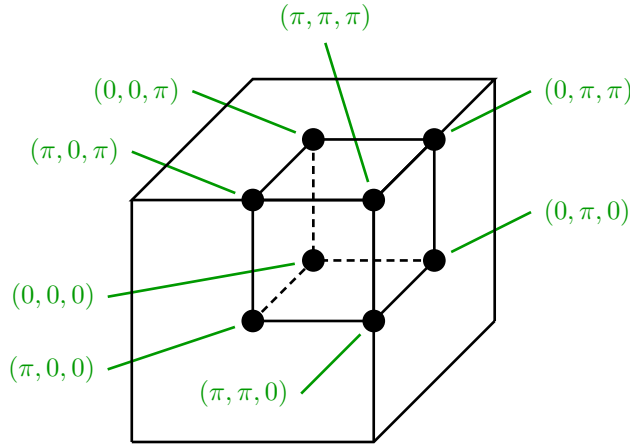


Figure 5.4: TRIMs of the three-dimensional Brillouin zone.

5.3 Complete classification

We now try to understand how one can put the above manipulations that lead to the \mathbb{Z}_2 index for TRI topological insulators into a bigger context. Let us review what (topological) classification schemes we already encountered. The first example was the characterization of a spin-1/2 in a magnetic field. There we discussed the geometric phase as a function of a smooth change in parameters of a Hamiltonian. The mathematical structure behind that was a fibre bundle. A fiber bundle is an object which locally looks like $M \times f$, where M is some base manifold and f the ‘‘fibre’’. For our case of the geometric phase, the base manifold was S^2 describing the parameter space of the ground state projector $|\psi_0\rangle\langle\psi_0|$. The fiber $f = U(1)$ was the phase of the ground state $|\psi_0\rangle$ that dropped out when we considered the projector. We have seen that one can classify such fibre bundles via a *Chern* number \mathcal{C} . For the example of a spin-1/2 in a magnetic field, the Chern number took the value $\mathcal{C} = -2\pi$. For the quantum Hall effect, we identified the fibre bundle with what looks locally like $T^2 \times U(1)$ where T^2 is the torus defined by the Aharonov Bohm fluxes through the openings of the (real space!) torus. We argued that also in this case the fibre bundle is characterized by the Chern number which can take any value in $2\pi\nu$ with $\nu \in \mathbb{Z}$ [6, 7].

We also considered special cases where the Aharonov-Bohm fluxes could be replaced by lattice momenta (k_x, k_y) . Moreover, in the simple case of a two-band Chern insulator the Chern number was shown to be equivalent to the Skyrmion number which characterizes mappings $T^2 \rightarrow S^2$ instead of fibre bundles. In general, we can hope to find the classification of mappings $T^d \rightarrow M$, where T^d is the d -dimensional Brillouin zone and M is some target manifold.

Attempting a topological classification of free fermion systems really means to define equivalence classes of first quantized Hamiltonians. Not so surprisingly, such equivalence classes depend strongly on the presence of symmetries: If we allow for arbitrary deformations of Hamiltonians

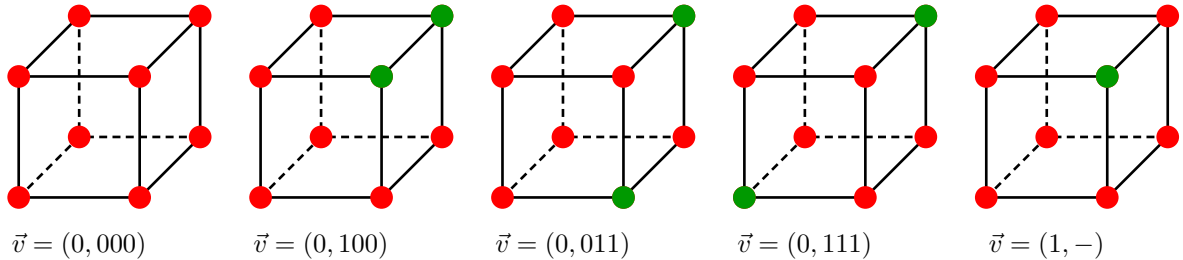


Figure 5.5: Stacking directions of 2D topological insulators.

(of course without the closing of the gap above the ground state!), we might be able to deform two Hamiltonians into each other that are distinct if we restrict the possible interpolation path by requiring symmetries.

A simple example of such a symmetry constraint is the following setup: Consider the restricted one-dimensional two-band system

$$H = \sum_i d_i(k) \sigma_i \quad \text{with} \quad \{H, \sigma_y\} = 0. \quad (5.27)$$

This symmetry requirement is identical with the demand that there is no y -component of the d -vector. In other words, the normalized d -vector lives on S^1 . Thanks to this restriction, or symmetry, each Hamiltonian in this class defines a mapping

$$S^1 \rightarrow S^1 \quad (5.28)$$

which is characterized by the winding number \mathcal{W} . In the absence of the symmetry $\{H, \sigma_y\}=0$, the d -vector could point anywhere on S^2 . Mappings

$$S^1 \rightarrow S^2 \quad (5.29)$$

are all trivial, however, as any closed one-dimensional path defined by the image of S^1 is smoothly contractible to a point. Hence, we cannot define a winding number in this case.

In the following we want to achieve three goals. First, we want to see how symmetries can influence the possible topological quantum numbers of band insulators. To this end we discuss three particular “symmetries” and see how they, together with the spatial dimension, give rise to a periodic table of topological insulators. The second goal will be to get the gist of what underlies the structure of the periodic table. The key ingredient will be the tool of dimensional reduction: We start with some topological quantum number (typically the Chern number) in some higher dimension. We then show how one can characterize families of lower-dimensional Hamiltonians obeying some symmetries using the higher dimensional topological number. Finally, our third goal is to be able to read the periodic table, find the right (hopefully simple) expression of the topological index and be able to calculate it. We will do so on three concrete examples in Sec. 5.4.

5.3.1 Anti-unitary symmetries

When we discuss symmetry constraints on possible equivalence relations between Hamiltonians we have to consider anti-unitary symmetries such as time reversal invariance with $\mathcal{T}i\mathcal{T}^{-1} = -i$. Unitary symmetries S that commute with the Hamiltonian $[H, S] = 0$ do not help us for the following reason: We simply go to combined eigenstates of both the symmetry S and the Hamiltonian. We want to assume that we only deal with such block-diagonal Hamiltonians from the outset. If we deal with anti-unitary symmetries, which do not have eigenstates, we cannot use this program of decomposing H into symmetric sub-blocks, however. The same holds for unitary symmetries S that anti-commute with the Hamiltonian, i.e., $\{H, S\} = 0$. We will see how such “symmetries” help us to classify topological insulators.

In the following we use a first quantized language where we write the single particle Hamiltonian as

$$H = \sum_{AB} \psi_A^\dagger \mathcal{H}_{AB} \psi_B, \quad (5.30)$$

where A, B run over all relevant quantum numbers. The object of interest is the matrix \mathcal{H}_{AB} . In case we deal with superconducting problems the corresponding matrix is constructed from the Nambu spinor

$$H = \sum_{AB} \begin{pmatrix} \psi_A^\dagger & \psi_{\bar{A}}^\dagger \end{pmatrix} \mathcal{H}_{AB} \begin{pmatrix} \psi_B \\ \psi_{\bar{B}}^\dagger \end{pmatrix}. \quad (5.31)$$

Here A and \bar{A} correspond to the paired quantum numbers: For example for an s -wave superconductor $A = (\mathbf{k}, \uparrow)$ and $\bar{A} = (-\mathbf{k}, \downarrow)$.

Time reversal

Let us now start with the anti-unitary time reversal symmetry

$$\mathcal{T} : \quad U_{\mathcal{T}}^{\dagger} \mathcal{H}^* U_{\mathcal{T}} = \mathcal{H}, \quad \text{with} \quad U_{\mathcal{T}}^{\dagger} U_{\mathcal{T}} = \mathbb{1}, \quad (5.32)$$

for some unitary rotation $U_{\mathcal{T}}$. Using the second quantized language we find for these matrices

$$\mathcal{T} \psi_A \mathcal{T}^{-1} = \sum_B [U_{\mathcal{T}}]_{AB} \psi_B. \quad (5.33)$$

Applying this identity twice, and making use of the fact that \mathcal{T} is anti-unitary, we find

$$\mathcal{T}^2 \psi_A \mathcal{T}^{-2} = \sum_B [U_{\mathcal{T}}^* U_{\mathcal{T}}]_{AB} \psi_B = \pm \psi_A, \quad \text{i.e.,} \quad U_{\mathcal{T}}^* U_{\mathcal{T}} = \pm \mathbb{1}. \quad (5.34)$$

Here we used that $\mathcal{T}^2 = -\mathbb{1}$ or $\mathcal{T}^2 = \mathbb{1}$, depending on whether we deal with systems of half-integer spins or not. The last equation can also be written as

$$U_{\mathcal{T}} = \pm U_{\mathcal{T}}^T. \quad (5.35)$$

Charge conjugation

The next (anti-) symmetry we consider is the charge-conjugation, or particle-hole symmetry

$$\mathcal{C} : \quad U_{\mathcal{C}}^{\dagger} \mathcal{H}^* U_{\mathcal{C}} = -\mathcal{H} \quad \text{with} \quad U_{\mathcal{C}}^{\dagger} U_{\mathcal{C}} = \mathbb{1}. \quad (5.36)$$

Where again we find $U_{\mathcal{C}}$ via

$$\mathcal{C} \psi_A \mathcal{C}^{-1} = \sum_B [U_{\mathcal{C}}^*]_{AB} \psi_B^{\dagger}. \quad (5.37)$$

And also in this case we can either have

$$U_{\mathcal{C}} = \pm U_{\mathcal{C}}^T, \quad (5.38)$$

depending on whether $\mathcal{C}^2 = \pm \mathbb{1}$. As this particle hole symmetry is slightly less standard than the time reversal symmetry we give two concrete examples. First, the Hamiltonian of an s -wave superconductor can be written as

$$H = \sum_k \begin{pmatrix} c_{k\uparrow} & c_{k\downarrow} & c_{-k\uparrow}^{\dagger} & c_{-k,\downarrow}^{\dagger} \end{pmatrix}^{\dagger} \underbrace{\begin{pmatrix} \xi(k) & 0 & 0 & \Delta_s \\ 0 & \xi(k) & -\Delta_s & 0 \\ 0 & -\Delta_s^* & -\xi(k) & 0 \\ \Delta_s^* & 0 & 0 & -\xi(k) \end{pmatrix}}_{\mathcal{H}_s} \begin{pmatrix} c_{k\uparrow} \\ c_{k\downarrow} \\ c_{-k\uparrow}^{\dagger} \\ c_{-k,\downarrow}^{\dagger} \end{pmatrix}. \quad (5.39)$$

This Hamiltonian has the anti-symmetry

$$U_{\mathcal{C}}^{\dagger} \mathcal{H}_s^* U_{\mathcal{C}} = -\mathcal{H}_s \quad \text{with} \quad U_{\mathcal{C}} = i\sigma_y \otimes \mathbb{1} \quad \text{and hence} \quad U_{\mathcal{C}} = -U_{\mathcal{C}}^T. \quad (5.40)$$

On the other hand, a triplet superconductor can be of the form

$$H = \sum_k \begin{pmatrix} c_{k\uparrow} & c_{k\downarrow} & c_{-k\uparrow}^{\dagger} & c_{-k,\downarrow}^{\dagger} \end{pmatrix}^{\dagger} \underbrace{\begin{pmatrix} \xi(k) & 0 & 0 & \Delta_t \\ 0 & \xi(k) & \Delta_t & 0 \\ 0 & \Delta_t^* & -\xi(k) & 0 \\ \Delta_t^* & 0 & 0 & -\xi(k) \end{pmatrix}}_{\mathcal{H}_t} \begin{pmatrix} c_{k\uparrow} \\ c_{k\downarrow} \\ c_{-k\uparrow}^{\dagger} \\ c_{-k,\downarrow}^{\dagger} \end{pmatrix}. \quad (5.41)$$

Now the Hamiltonian has the anti-symmetry

$$U_{\mathcal{C}}^{\dagger} \mathcal{H}_t^* U_{\mathcal{C}} = -\mathcal{H}_t \quad \text{with} \quad U_{\mathcal{C}} = \sigma_x \otimes \mathbb{1} \quad \text{and hence} \quad U_{\mathcal{C}} = U_{\mathcal{C}}^T. \quad (5.42)$$

Note, that all Bogoliubov-de Gennes (BdG) Hamiltonians of mean-field superconductors have a \mathcal{C} -type symmetry built in by construction (via the Nambu formalism).

Chiral symmetry

One more option is for the Hamiltonian to posses the following anti-symmetry

$$\mathcal{S} : \quad U_{\mathcal{S}}^\dagger \mathcal{H} U_{\mathcal{S}} = -\mathcal{H} \quad \text{with} \quad U_{\mathcal{S}}^\dagger U_{\mathcal{S}} = \mathbb{1}. \quad \text{and} \quad U_{\mathcal{S}}^2 = \mathbb{1}. \quad (5.43)$$

This symmetry is called chiral or *sub-lattice* symmetry as it often occurs on bipartite lattice models. Note, that whenever the system has a chiral symmetry and either a particle-hole or time-reversal, it actually posses all three of them (show!).

5.3.2 The periodic table

Let us now classify all possible symmetry classes according to the above three “symmetries”. For the time-reversal and particle-hole symmetry we have three options. Either there is no symmetry, one that squares to $\mathbb{1}$, or one that squares to $-\mathbb{1}$. We denote these cases with $0, 1, -1$. Together, there are $3 \times 3 = 9$ different options. Turning around the argument above that a \mathcal{C} (\mathcal{T}) together with an \mathcal{S} type symmetry implies a \mathcal{T} (\mathcal{C}) symmetry we see that $\mathcal{S} = \mathcal{C} \circ \mathcal{T}$. Therefore, for all cases where either \mathcal{T} or \mathcal{C} are present the presence or absence of \mathcal{S} is fixed. Only if both particle-hole and time-reversal symmetry are absent, \mathcal{S} can be either present (1) or absent (0). This yields in total 10 different symmetry classes. In a series of papers Kitaev [8] and Ludwig and co-workers [9, 10] classified all possible topological indices given the symmetry class and the spatial dimension. We summarize their results in Tab. 5.1.

label	symmetry												spatial dimension			
	\mathcal{T}	\mathcal{C}	\mathcal{S}	$d = 1$	$d = 2$	$d = 3$	$d = 4$	$d = 5$	$d = 6$	$d = 7$	$d = 8$	\dots	$d = 1$	$d = 2$	$d = 3$	$d = 4$
the complex cases:																
A	0	0	0	0	\mathbb{Z}	0	\mathbb{Z}	0	\mathbb{Z}	0	\mathbb{Z}	\dots	0	\mathbb{Z}_2	\mathbb{Z}_2	\mathbb{Z}
AIII	0	0	1	\mathbb{Z}	0	\mathbb{Z}	0	\mathbb{Z}	0	\mathbb{Z}	0	\dots	0	\mathbb{Z}_2	0	\dots
the real cases:																
AI	1	0	0	0	0	0	$2\mathbb{Z}$	0	\mathbb{Z}_2	\mathbb{Z}_2	\mathbb{Z}	\dots	0	\mathbb{Z}_2	\mathbb{Z}_2	\mathbb{Z}
BDI	1	1	1	\mathbb{Z}	0	0	0	$2\mathbb{Z}$	0	\mathbb{Z}_2	\mathbb{Z}_2	\dots	0	\mathbb{Z}_2	\mathbb{Z}_2	\mathbb{Z}
D	0	1	0	\mathbb{Z}_2	\mathbb{Z}	0	0	0	$2\mathbb{Z}$	0	\mathbb{Z}_2	\dots	0	\mathbb{Z}_2	\mathbb{Z}_2	\mathbb{Z}
DIII	-1	1	1	\mathbb{Z}_2	\mathbb{Z}_2	\mathbb{Z}	0	0	0	$2\mathbb{Z}$	0	\dots	0	\mathbb{Z}_2	\mathbb{Z}_2	\mathbb{Z}
AII	-1	0	0	0	\mathbb{Z}_2	\mathbb{Z}_2	\mathbb{Z}	0	0	0	$2\mathbb{Z}$	\dots	0	\mathbb{Z}_2	\mathbb{Z}_2	\mathbb{Z}
CII	-1	-1	1	$2\mathbb{Z}$	0	\mathbb{Z}_2	\mathbb{Z}_2	\mathbb{Z}	0	0	0	\dots	0	0	0	\mathbb{Z}
C	0	-1	0	0	$2\mathbb{Z}$	0	\mathbb{Z}_2	\mathbb{Z}_2	\mathbb{Z}	0	0	\dots	0	0	0	\mathbb{Z}
CI	1	-1	1	0	0	$2\mathbb{Z}$	0	\mathbb{Z}_2	\mathbb{Z}_2	\mathbb{Z}	0	\dots	0	\mathbb{Z}_2	\mathbb{Z}_2	\mathbb{Z}

Table 5.1: Periodic table of topological insulators and superconductors. \mathbb{Z}_2 and \mathbb{Z} denote binary and integer topological indices, respectively. $2\mathbb{Z}$ denotes an even integer. The symmetries \mathcal{T} , \mathcal{C} and $\mathcal{S} = \mathcal{T} \circ \mathcal{C}$ are explained in the text. A zero denotes the absence of the symmetry and for \mathcal{T} and \mathcal{C} , the ± 1 indicates if these symmetries square to $\pm \mathbb{1}$.

One observes an obvious 8-fold symmetry in the direction of the spatial dimension. The explanation of this repetition lies beyond the scope of this course. However, as dimensional reduction plays a key role in the derivation of Tab. 5.1, we present on such step for the case of symmetry class D, going from $d = 2 \rightarrow 1$. Before we do so, it is worth mentioning, that from a applicative point of view, our standard job will be to:

1. Identify the symmetries and with that the class A, AI, AII, AIII, BDI, etc.

2. Check in Tab. 5.1 if for the given symmetry class and spatial dimension there can be a topologically non-trivial state.
3. Go to the paper by Ryu et al. [9].
4. Find the explicit formula for the respective index.
5. Compute it.

5.3.3 Dimensional reduction

This section is following the derivation in Ref. [11].

Our goal is to take the step of dimensional reduction to relate the \mathbb{Z} index of symmetry class D in three dimensions to the \mathbb{Z}_2 index of the same symmetry class in one spatial dimension. In this section. We consider one dimensional lattice systems where the Hamiltonian matrix fulfills

$$U_C^\dagger \mathcal{H}^*(-k) U_C = \mathcal{H}(k) \quad \text{with} \quad U_C = U_C^T. \quad (5.44)$$

We now try to establish an equivalence relation between two such Hamiltonians $\mathcal{H}_1(k)$ and $\mathcal{H}_2(k)$. To borrow the Chern number from one dimension higher, we construct a path, or interpolation $\mathcal{H}(k, \vartheta)$, with $\vartheta \in [0, \pi]$ connecting the two Hamiltonians

$$\mathcal{H}(k, 0) = \mathcal{H}_1(k) \quad \text{and} \quad \mathcal{H}(k, \pi) = \mathcal{H}_2(k). \quad (5.45)$$

In general, the Hamiltonian for an arbitrary $\vartheta \in [0, \pi]$ will not posses the symmetry (5.44). We correct for this by explicitly constructing the cyclic interpolation for $\vartheta \in [\pi, 2\pi]$

$$\mathcal{H}(k, \vartheta) = -U_C^\dagger \mathcal{H}^*(-k, 2\pi - \vartheta) U_C. \quad (5.46)$$

Interpreted as a two-dimensional problem, $H(k, \vartheta)$ is now manifestly particle-hole symmetric. By requiring for the whole interpolation the system to be gapped we can define the Chern number of this cyclic interpolation¹

$$C_H = \oint d\vartheta \frac{\partial P(\vartheta)}{\partial \vartheta}, \quad (5.49)$$

¹ To see that these formula indeed corresponds to our known result we first state that (we drop the label and sum over n for simplicity)

$$\begin{aligned} \mathcal{F}_{\vartheta k} &= \partial_\vartheta i\langle \varphi_k | \partial_k \varphi_k \rangle - \partial_k i\langle \varphi_k | \partial_\vartheta \varphi_k \rangle = i\langle \partial_\vartheta \varphi_k | \partial_k \varphi_k \rangle + i\langle \varphi_k | \partial_\vartheta \partial_k \varphi_k \rangle - i\langle \partial_k \varphi_k | \partial_\vartheta \varphi_k \rangle - i\langle \varphi_k | \partial_k \partial_\vartheta \varphi_k \rangle \\ &= i\langle \partial_\vartheta \varphi_k | \partial_k \varphi_k \rangle - i\langle \partial_k \varphi_k | \partial_\vartheta \varphi_k \rangle. \end{aligned}$$

We now write

$$\begin{aligned} \oint d\vartheta \frac{\partial P(\vartheta)}{\partial \vartheta} &= \oint d\vartheta \frac{\partial}{\partial \vartheta} \oint \frac{dk}{2\pi} i\langle \varphi_k | \partial_k \varphi_k \rangle = \oint d\vartheta \oint \frac{dk}{2\pi} (i\langle \partial_\vartheta \varphi_k | \partial_k \varphi_k \rangle + i\langle \varphi_k | \partial_\vartheta \partial_k \varphi_k \rangle) \\ &\stackrel{\text{P.I.}}{=} \oint d\vartheta \oint \frac{dk}{2\pi} (i\langle \partial_\vartheta \varphi_k | \partial_k \varphi_k \rangle - i\langle \partial_k \varphi_k | \partial_\vartheta \varphi_k \rangle) + \oint d\vartheta i\langle \underbrace{\varphi_{k=2\pi} | \partial_\vartheta \varphi_{k=2\pi}}_{\mathcal{A}_\vartheta(k=2\pi)} \rangle + \oint d\vartheta i\langle \underbrace{\varphi_{k=0} | \partial_\vartheta \varphi_{k=0}}_{\mathcal{A}_\vartheta(k=0)} \rangle. \end{aligned}$$

From the discussion of fiber bundles we know that we cannot necessarily choose a smooth gauge such that \mathcal{A} is a single-valued function over the whole torus. However, we can always choose a gauge where \mathcal{A}_ϑ is single valued (akin the Landau gauge for the electro-magnetic gauge potential). For such a gauge the integrals

$$\oint d\vartheta \mathcal{A}_\vartheta(k) = 0 \quad (5.47)$$

for both $k = 0$ and $k = 2\pi$. With this we established

$$\oint d\vartheta \frac{\partial P(\vartheta)}{\partial \vartheta} = \oint d\vartheta \oint \frac{dk}{2\pi} (i\langle \partial_\vartheta \varphi_k | \partial_k \varphi_k \rangle - i\langle \partial_k \varphi_k | \partial_\vartheta \varphi_k \rangle) = \frac{1}{2\pi} \oint d\vartheta \oint dk \mathcal{F}_{\vartheta k} = C, \quad (5.48)$$

as we tried to prove.

where as before we defined the charge polarization as a function of the pumping parameter ϑ

$$P(\vartheta) = \oint \frac{dk}{2\pi} \sum_{n \text{ filled}} i \langle \varphi_{nk} | \partial_k \varphi_{nk} \rangle \quad (5.50)$$

To make further progress in establishing an equivalence relation between one dimensional Hamiltonians of class D we note that owing to the particle-hole symmetry, eigenstates of different locations in the Brillouin zone are related to each other. Without showing the full algebraic manipulations [11], we state that

$$P(\vartheta) = -P(2\pi - \vartheta). \quad (5.51)$$

An immediate consequence is

$$\int_0^\pi d\vartheta P(\vartheta) = \int_\pi^{2\pi} d\vartheta P(\vartheta). \quad (5.52)$$

We remind ourselves that these two equations rely crucially on the presence of the particle-hole symmetry. Consider now another particle-hole symmetric interpolation $\mathcal{H}'(k, \vartheta)$ between $\mathcal{H}_1(k)$ and $\mathcal{H}_2(k)$. We denote the corresponding polarization with $P'(\vartheta)$. The relative Chern number of the two interpolations is then given by

$$\mathcal{C}_{\mathcal{H}} - \mathcal{C}_{\mathcal{H}'} = \oint d\vartheta \left(\frac{\partial P(\vartheta)}{\partial \vartheta} - \frac{\partial P'(\vartheta)}{\partial \vartheta} \right). \quad (5.53)$$

One can define two yet different interpolations $\mathcal{G}_1(k, \vartheta)$ and $\mathcal{G}_2(k, \vartheta)$ (not particle-hole symmetric!) via

$$\mathcal{G}_1(k, \vartheta) = \begin{cases} \mathcal{H}(k, \vartheta) & \vartheta \in [0, \pi] \\ \mathcal{H}'(k, 2\pi - \vartheta) & \vartheta \in [\pi, 2\pi] \end{cases}, \quad (5.54)$$

and

$$\mathcal{G}_2(k, \vartheta) = \begin{cases} \mathcal{H}'(k, 2\pi - \vartheta) & \vartheta \in [0, \pi] \\ \mathcal{H}(k, \vartheta) & \vartheta \in [\pi, 2\pi] \end{cases}. \quad (5.55)$$

These interpolations are shown in Fig. 5.6. We see that \mathcal{G}_1 is obtained by reconnecting \mathcal{H} and \mathcal{H}' such that it always runs in the upper half-space and vice-versa for \mathcal{G}_2 . It is straightforward to see that

$$\mathcal{C}_{\mathcal{G}_1} = \int_0^\pi d\vartheta \left(\frac{\partial P(\vartheta)}{\partial \vartheta} - \frac{\partial P'(\vartheta)}{\partial \vartheta} \right), \quad (5.56)$$

and

$$\mathcal{C}_{\mathcal{G}_2} = \int_\pi^{2\pi} d\vartheta \left(\frac{\partial P(\vartheta)}{\partial \vartheta} - \frac{\partial P'(\vartheta)}{\partial \vartheta} \right). \quad (5.57)$$

From this it is easy to see that $\mathcal{C}_{\mathcal{H}} - \mathcal{C}_{\mathcal{H}'} = \mathcal{C}_{\mathcal{G}_1} + \mathcal{C}_{\mathcal{G}_2}$. Moreover, if we use the symmetry (5.52) we see that $\mathcal{C}_{\mathcal{G}_1} = \mathcal{C}_{\mathcal{G}_2}$ and hence

$$\mathcal{C}_{\mathcal{H}} - \mathcal{C}_{\mathcal{H}'} = 2\nu \quad \text{with} \quad \nu \in \mathbb{Z}. \quad (5.58)$$

How can we understand this result? Remember that each interpolation gives rise to a two-dimensional band-structure. The Chern number of this band-structure, $\mathcal{C}_{\mathcal{H}}$ can only change if when going from $\mathcal{H} \rightarrow \mathcal{H}'$ we close a gap. However, due to the particle-hole symmetry, such gap closings always occur in two points in the Brillouin zone, see Fig. 5.6. Therefore, for all possible interpolations between our original one dimensional problems $\mathcal{H}_1(k)$ and $\mathcal{H}_2(k)$ the parity of the Chern number is conserved. We can thus write the *relative Chern parity*

$$N[\mathcal{H}_1(k), \mathcal{H}_2(k)] = (-1)^{\mathcal{C}_{\mathcal{H}(k, \vartheta)}}. \quad (5.59)$$

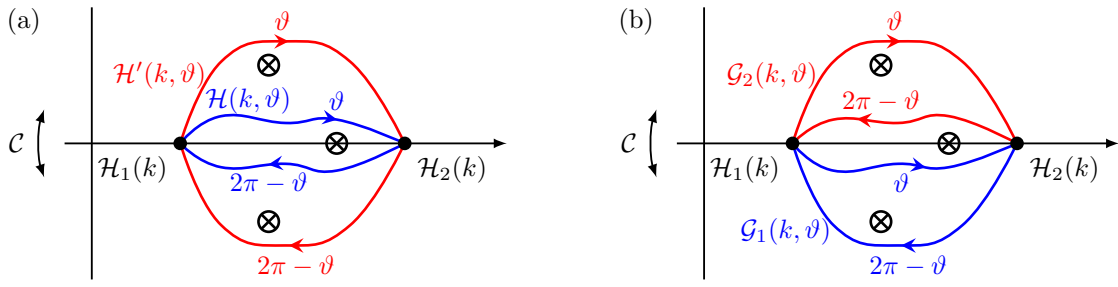


Figure 5.6: (a) Interpolation between two particle-hole symmetric one dimensional Hamiltonians $\mathcal{H}_{1/2}(k)$. Along the horizontal axis we move between different one-dimensional Hamiltonians. Along the vertical axis, the particle-hole symmetry operation on the one-dimensional Hamiltonians corresponds to a mirroring around the horizontal axis. Hence, we see that the blue (red) interpolation paths are constructed such that the interpolation, interpreted as a two-dimensional Hamiltonian, is manifestly symmetric under \mathcal{C} . The crosses correspond to gap closings in $\mathcal{H}(k, \vartheta)$ and hence the interpolations are not allowed to touch them in order for $\mathcal{H}(k, \vartheta)$ to have a well defined Chern number. Due to symmetry constraints, all gap closings away from the particle-hole symmetric line appear in pairs. Consequently, we might change the Chern number by deforming the interpolation, but always by two. Hence, independently of how $\mathcal{H}_1(k)$ and $\mathcal{H}_2(k)$ are connected, the Chern number parity is independent of the interpolation and hence can be used as a \mathbb{Z}_2 index. (b) Different interpolation paths to make the arguments in (a) formal.

It is easy to prove that this relative Chern parity has the property

$$N[\mathcal{H}_1(k), \mathcal{H}_2(k)]N[\mathcal{H}_2(k), \mathcal{H}_3(k)] = N[\mathcal{H}_1(k), \mathcal{H}_3(k)] \quad (5.60)$$

and consequently defines an equivalence relation. Equivalence classes are given by Hamiltonians in symmetry class D which have the same relative Chern parity. We can moreover define an absolute \mathbb{Z}_2 index by choosing a naturally ‘‘trivial’’ Hamiltonian \mathcal{H}_0 and then define

$$\mathcal{H}(k) \in D \text{ trivial} \Leftrightarrow N[\mathcal{H}(k), \mathcal{H}_0] = 1, \quad (5.61)$$

$$\mathcal{H}(k) \in D \text{ non-trivial:} \Leftrightarrow N[\mathcal{H}(k), \mathcal{H}_0] = -1. \quad (5.62)$$

While the above developments might appear somewhat formal, they have a direct physical consequence. Imagine a one dimensional system \mathcal{H}_{nt} which is non-trivial according to (5.62). The two dimensional system given by the interpolation between \mathcal{H}_0 and \mathcal{H}_{nt} therefore has an odd Chern number and correspondingly an odd number of surface modes traversing the gap on each side of a finite cylinder. Let us imagine ϑ to be the momentum along the edge of the cylinder. Due to the particle hole symmetry between ϑ and $2\pi - \vartheta$, zero levels always appear in pairs at ϑ and $2\pi - \vartheta$. As we need an odd number of them, there has to be one either at $\vartheta = 0$ or π . As $\vartheta = 0$ corresponds to the trivial atomic Hamiltonian \mathcal{H}_0 , there are no end states at $\vartheta = 0$. In other words, a non-trivial \mathbb{Z}_2 index in class D guarantees the existence of zero energy end states for a one dimensional system with an end.

This concludes our discussion of the structure of the periodic table 5.1. We have seen on one concrete example how a Chern number of a higher-dimensional member of a symmetry class can give rise to a \mathbb{Z}_2 index in one dimension lower. We refer the interested reader to the publications by Ryu et al. [9] and Kitaev [8] for further details. Instead of pursuing the study of what lies behind the periodic table further, we move to the discussion of three prototypical models of topological free fermion systems. One important void owing to this strategy is that we did not discuss topological field theories that describe the electro-magnetic response of topological insulators. For this we need a bit more technical tools which we will develop before we discuss the fractional quantum Hall effect. Once we are acquainted with these tools we will come back to this issue.

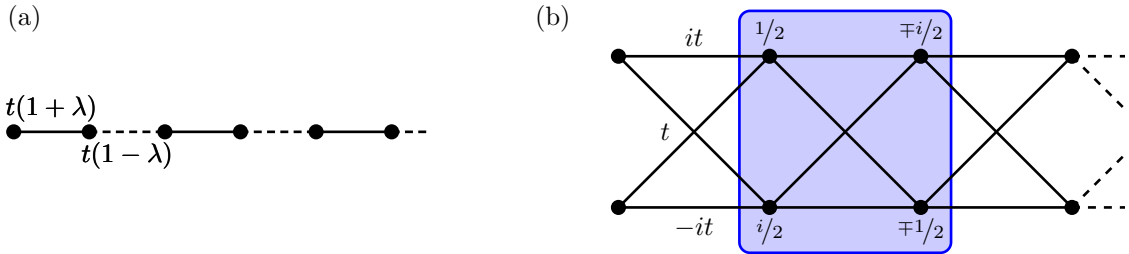


Figure 5.7: (a) The Su-Schrieffer-Heeger model. (b) Localized eigenstate in the flat band Creutz model.

5.4 Examples of topological free fermion systems

5.4.1 Su-Schrieffer-Heeger and Creutz model

In this section we discuss a simple one dimensional hopping model originally introduced by Su, Schrieffer and Heeger (SSH) to describe certain aspects of polyacetylene [12]. Consider the following tight binding model

$$H = -t \sum_i [(-1)^i \lambda + 1] c_i^\dagger c_{i+1} + \text{H.c.} \quad \Rightarrow \quad \mathcal{H}(k) = -t \sum_i d_i(k) \sigma_i, \quad (5.63)$$

with

$$d_x(k) = 2 \cos(k), \quad d_y(k) = 2\lambda \sin(k), \quad d_z(k) = 0. \quad (5.64)$$

If we rotate the d -vector, the structure of the problem does not change. However, we will see that the physical interpretation of the model can be quite different and is then known as the Creutz ladder [13], cf. Fig. 5.7. We rotate by $\pi/2$ around the x -axis to obtain

$$d_x(k) = 2 \cos(k), \quad d_y(k) = 0, \quad d_z(k) = 2\lambda \sin(k). \quad (5.65)$$

As the d -vector does not contain a y -component, we immediately conclude that $\{\mathcal{H}, \sigma_y\} = 0$ with $\sigma_y^2 = \mathbb{1}$, i.e., we have a chiral symmetry. Moreover, the Hamiltonian has the property

$$\mathcal{H}^*(k) = \mathcal{H}(k) = -\sigma_z \mathcal{H}(-k) \sigma_z \quad (5.66)$$

which we identify as a particle hole symmetry with $U_C = \sigma_z$. Hence, we also have a time reversal symmetry with $U_T = U_C^{-1} U_S = \sigma_z \sigma_y = -i \sigma_x$. We see that both $U_{C/T} = U_{C/T}^T$ and hence both T and C square to one, which puts us in symmetry class BDI. Consulting Tab. 5.1, we expect a \mathbb{Z} quantum number. Note, however, that we can break either (and hence both) particle-hole or time-reversal symmetry and we end up in class AIII, which is again described by a \mathbb{Z} topological index. We therefore consult the Ryu paper [9] for class AIII. From Ref. [9] we learn that we should consider the projector onto the ground state $|v_-(k)\rangle$

$$P(k) = |v_-(k)\rangle \langle v_-(k)| = \frac{1}{2} [\mathbb{1} - \bar{Q}(k)] = \left[\frac{1}{2} \mathbb{1} - \frac{1}{2} \mathbf{d}(k) \boldsymbol{\sigma} \right]. \quad (5.67)$$

Due to the chiral symmetry, the \bar{Q} -matrix can be brought in off-diagonal form in the eigen-basis of the S -symmetry, i.e.,

$$\begin{aligned} Q(k) &= \frac{1}{2} \begin{pmatrix} -i & 1 \\ i & 1 \end{pmatrix} \bar{Q}(k) \begin{pmatrix} i & -i \\ 1 & 1 \end{pmatrix} = \begin{pmatrix} 0 & q(k) \\ q^*(k) & 0 \end{pmatrix} \\ &= \begin{pmatrix} 0 & -\lambda \sin(k) - i \cos(k) \\ -\lambda \sin(k) + i \cos(k) & 0 \end{pmatrix}. \end{aligned} \quad (5.68)$$

The winding number density is now given by [9]

$$w(k) = iq^{-1}(k)\partial_k q(k) = \frac{i\lambda \cos(k) + \sin(k)}{i\cos(k) + \lambda \sin(k)} = \begin{cases} 1 & \lambda = 1, \\ -1 & \lambda = -1. \end{cases} \quad (5.69)$$

As the gap is closing only at $\lambda = 0$, the two special values $\lambda = \pm 1$ suffice for the calculation of the total winding number in the two distinct phases

$$\mathcal{W} = \int_{-\pi}^{\pi} \frac{dk}{2\pi} w(k) = \begin{cases} 1 & \lambda > 0, \\ -1 & \lambda < 0. \end{cases} \quad (5.70)$$

What does this winding number signify? From expression (5.67), it is clear that it corresponds to the winding of the d -vector throughout the Brillouin zone. However, we know, that the spinor-wave function of a spin-1/2 only returns to itself after a rotation by 4π . To investigate this further, let us specialize to $\lambda = 1$ for simplicity. In this case, the dispersion reduces to

$$|\mathbf{d}(k)| = \pm 2, \quad (5.71)$$

i.e., we deal with two completely flat bands. In the case of the SSH model, this is somewhat trivial, as we cut the chain into a set of independent dimers. For the Creutz ladder, this indicates a rather delicate interference effect, see Fig. 5.7! The ground state wave function can be explicitly written as

$$|v_{-}(k)\rangle = \begin{pmatrix} \cos[(\pi - 2k)/4] \\ -\sin[(\pi - 2k)/4] \end{pmatrix} \quad \text{with} \quad |v_{-}(-\pi)\rangle = -|v_{-}(\pi)\rangle. \quad (5.72)$$

Hence, we see that indeed the winding number \mathcal{W} is responsible for a phase jump of π at the Brillouin zone-boundary. We try to see what this means for the Wannier functions

$$W_{\alpha,-}(l) = \int_{-\pi}^{\pi} \frac{dk}{2\pi} v_{\alpha,-}(k) e^{ikl}, \quad (5.73)$$

where α is the sub-lattice index label. Let us see what we can deduce from the presence of non-trivial winding number

$$\begin{aligned} W_{\alpha,-}(l) &= \int_{-\pi}^{\pi} \frac{dk}{2\pi} v_{\alpha,-}(k) e^{ikl} = \frac{1}{2\pi il} \langle v_{\alpha,-}(k) e^{ikl} \rangle \Big|_{k=-\pi, \pi} - \frac{1}{il} \int_{-\pi}^{\pi} \frac{dk}{2\pi} v'_{\alpha,-}(k) e^{ikl} \\ &= \frac{(-1)^l \Delta v_{\alpha,-}}{2\pi il} + \frac{1}{2\pi l^2} \langle v'_{\alpha,-}(k) e^{ikl} \rangle \Big|_{k=-\pi, \pi} - \frac{1}{l^2} \int_{-\pi}^{\pi} \frac{dk}{2\pi} v''_{\alpha,-}(k) e^{ikl} = \\ &= \frac{(-1)^l}{2\pi} \left[\frac{\Delta v_{\alpha,-}}{il} + \frac{\Delta v'_{\alpha,-}}{l^2} - \frac{\Delta v''_{\alpha,-}}{il^3} + \mathcal{O}(1/l^4) \right]. \end{aligned} \quad (5.74)$$

We make the following two observations. (i) If $\mathcal{W} = 0$, all the discontinuities $\Delta v_{\alpha,-}^{(n)} \equiv 0$. This was to be expected as in this case we know that the Wannier functions are exponentially localized [14] and hence have an essential singularity at $1/l \rightarrow 0$. (ii) If $\mathcal{W} = \pm 1$, $v_{\alpha,-}(k)$ is a 4π -periodic function and generically has non-zero $\Delta v_{\alpha,-}(k)$ and therefore

$$w_{\alpha\nu}(l) \xrightarrow{l \rightarrow \infty} \frac{1}{l}. \quad (5.75)$$

(iii) For an even winding number, there is no such discontinuity. For our problem of the Creutz ladder we deduce from the above considerations that the large- l behavior is given by

$$W_{\alpha,-}(l) \sim \frac{-i}{\sqrt{2}\pi l}. \quad (5.76)$$

This result is in accordance with the full expression

$$W_{\alpha,-}(l) = \frac{\sqrt{2}(-1)^l(-1 \pm 2il)}{\pi(4l^2 - 1)}. \quad (5.77)$$

Instead of site-centered, we can use bond centered Wannier functions for the lower band

$$W_{\alpha,-}^{\text{bond}}(l) = \int_{-\pi}^{\pi} \frac{dk}{2\pi} v_{\alpha,-}(k) e^{ik(l+1/2)} = \begin{cases} \frac{1+i}{2\sqrt{2}} \delta_{l,-1} + \frac{1-i}{2\sqrt{2}} \delta_{l,0} & \alpha = 1, \\ -\frac{1-i}{2\sqrt{2}} \delta_{l,-1} - \frac{1+i}{2\sqrt{2}} \delta_{l,0} & \alpha = 2. \end{cases} \quad (5.78)$$

These states are not only exponentially but strictly localized to one bond! How can we reconcile this with the above result that Wannier functions have an $1/l$ -tail? To see this, we make the following observation: In the form we wrote the eigenstates $|v_-(k)\rangle$ we made a certain gauge choice. We are free to choose a different one. Led by the above observation that the bond centered Wannier function are localized, we make an explicitly gauge transformation

$$|v_-(k)\rangle \longrightarrow |\tilde{v}_-(k)\rangle = e^{ik/2} |v_-(k)\rangle = \begin{pmatrix} e^{ik/2} \cos[(\pi - 2k)/4] \\ -e^{ik/2} \sin[(\pi - 2k)/4] \end{pmatrix}, \quad (5.79)$$

with the property

$$|\tilde{v}_-(-\pi)\rangle = |\tilde{v}_-(\pi)\rangle. \quad (5.80)$$

Using this gauge, it becomes clear that there are no non-vanishing terms in the $1/l$ expansion of the Wannier function. This is a very deep truth: If there is no obstruction to a smooth gauge for the Bloch wave functions, Wannier functions can be localized (at least) exponentially. Also the opposite statement is true: If there is an obstruction to a smooth gauge, we cannot localize the Wannier functions. As we know that the Chern number exactly signals such an impossibility to choose a smooth gauge. From this we deduce that in a Chern insulator the Wannier functions can never be localized!

5.4.2 Kitaev wire

In this section we discuss Kitaev's toy model for a spinless p -wave superconducting chain described by

$$H = -\mu \sum_{i=1}^N c_i^\dagger c_i - \sum_{i=1}^{N-1} \left(t c_i^\dagger c_{i+1} + e^{i\varphi} \Delta c_i c_{i+1} + \text{H.c.} \right). \quad (5.81)$$

Here, N is the number of sites, μ the chemical potential, and t and Δ the hopping and pairing amplitude, respectively. If we write the same Hamiltonian in momentum space we find

$$H = \frac{1}{2} \sum_k \begin{pmatrix} c_k & c_{-k}^\dagger \end{pmatrix}^\dagger \underbrace{\begin{pmatrix} -t \cos(k) - \mu & e^{i\varphi} \Delta \sin(k) \\ -e^{-i\varphi} \Delta \sin(k) & t \cos(k) + \mu \end{pmatrix}}_{\mathcal{H}_k} \begin{pmatrix} c_k \\ c_{-k}^\dagger \end{pmatrix} \quad \text{with} \quad \mathcal{H}_k = \sum_i d_i(k) \sigma_i,$$

where the d -vector is given by

$$d_x(k) = \sin(\varphi) \Delta \sin(k), \quad (5.82)$$

$$d_y(k) = \cos(\varphi) \Delta \sin(k), \quad (5.83)$$

$$d_z(k) = -t \cos(k) - \mu. \quad (5.84)$$

As we are dealing with a BdG problem, the particle hole symmetry is built in with a $U_C = \sigma_x$. $U_C = U_C^\dagger$ as expected for a triplet superconductor. It is a bit more involved to determine if there is also an \mathcal{S} symmetry (and consequently also time reversal). A little exercise shows that

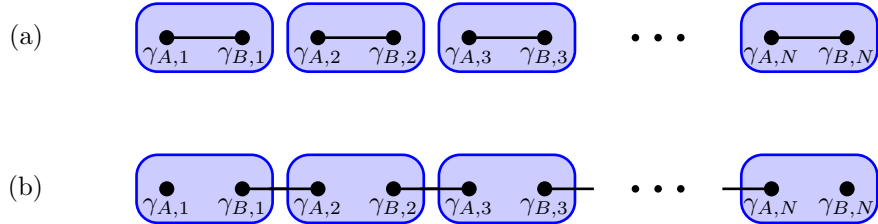


Figure 5.8: (a) Eigenstates for the Kitaev wire for $\mu < 0$ and $t = \Delta = 0$. (b) The same for $\mu > 0$, and $\Delta = t \neq 0$.

for $\varphi = 0$, $\sigma_x \mathcal{H}(k) \sigma_x = -\mathcal{H}(k)$. Hence, we only need to transform away the phase φ of the superconducting order parameter. This can be done via

$$r(\varphi) = \cos(\varphi/2)\mathbb{1} + i \sin(\varphi/2)\sigma_z. \quad (5.85)$$

With this find an S -symmetry with $U_S = r(\varphi)\sigma_x$. As a by-product, the time-reversal symmetry is established for a unitary $U_T = U_C^{-1}U_S = \sigma_x r(\varphi)\sigma_x = r(-\varphi)$. A quick look at Tab. 5.1 tells us that we are in symmetry class BDI characterized by a \mathbb{Z} index. Owing to the rotation $r(\varphi)$, which does not depend on k , it is clear that we can use the winding number of chiral systems to obtain this index. However, we want to anticipate a potential breaking of time reversal invariance. In this case we deal with a class D-problem for which we established the relative Chern parity as a good topological index. Recall that the relative Chern parity is obtained by assuming $\mathcal{H}(k)$ to be the $k_y = \pi$ cut of a two-dimensional Hamiltonian. As a reference we took for $k_y = 0$ a trivial reference state. Owing to the fact that we deal with a two-band system we obtain the Chern number from the Skyrmion number (4.9). However, we know that along $k_y = 0$ the d -vector can be chosen to point constantly in positive z -direction. Moreover, the particle-hole symmetry forces

$$d_x(0) = d_y(0) = d_x(\pi) = d_y(\pi) = 0. \quad (5.86)$$

Hence, in order for the Chern number of the interpolation path to be odd, we need (show!)

$$\frac{d_z(0)}{|d_z(0)|} \frac{d_z(\pi)}{|d_z(\pi)|} = s_0 s_\pi = \nu < 0. \quad (5.87)$$

For the present case, this means we require

$$\nu = -(t - \mu)(t + \mu) < 0 \quad \Rightarrow \quad |\mu| < t. \quad (5.88)$$

Let us see what this index means for a finite system with edges. To this end it is convenient to introduce two *real fermions* per site

$$c_i = \frac{e^{i\varphi}}{2} (\gamma_{iA} + i\gamma_{iB}) \quad \text{with the properties} \quad \gamma_{i\alpha}^\dagger = \gamma_{i\alpha} \quad \text{and} \quad \{\gamma_{i\alpha}, \gamma_{j\beta}\} = 2\delta_{\alpha\beta}\delta_{ij}. \quad (5.89)$$

In these new real, or *Majorana*, fermions the Hamiltonian reads

$$H = -\frac{\mu}{2} \sum_{i=1}^N (1 + i\gamma_{iA}\gamma_{iB}) - \frac{i}{4} \sum_{i=1}^{N-1} [(\Delta + t)\gamma_{iB}\gamma_{i+1A} + (\Delta - t)\gamma_{iA}\gamma_{i+1B}]. \quad (5.90)$$

Let us consider two special points in the phase diagram. For the topologically trivial region we choose $\mu < 0$ and $\Delta = t = 0$. In this case the Hamiltonian is trivial and it is clear that in order

to write in terms of complex fermions again, we just revert procedure (5.89), cf. Fig 5.8. For the topologically non-trivial case we choose $\mu = 0$ and $\Delta = t \neq 0$. The Hamiltonian now reduces to

$$H = -\frac{i}{2}t \sum_{i=1}^{N-1} \gamma_{iB}\gamma_{i+1A}. \quad (5.91)$$

We make two observations: (i) The Majorana operators γ_{1A} and γ_{NB} do not appear in the Hamiltonian. (ii) We can go back to a fermionic representation by “paring” Majorana fermions over bonds

$$d_i = \frac{1}{2}(\gamma_{i+1A} + i\gamma_{iB}). \quad (5.92)$$

Written in these fermions the Hamiltonian is again strikingly simple

$$H = t \sum_{i=1}^{N-1} \left(d_i^\dagger d_i + \frac{1}{2} \right). \quad (5.93)$$

Clearly, the d_i -fermions are the quasi-particle excitations above the superconducting ground state. However, owing to the fact that γ_{1A} and γ_{NB} did not appear in the Hamiltonian, we can form another fermion, see Fig 5.8

$$f = \frac{1}{2}(\gamma_{1A} + i\gamma_{NB}). \quad (5.94)$$

This f -fermion formed out of the Majorana modes at the two edges does not appear in the Hamiltonian. Therefore, the ground state is doubly degenerate: If $f|0\rangle = 0$ is a ground state, also $|1\rangle = f^\dagger|0\rangle$ is.

5.4.3 Two dimensional $p_x + ip_y$ superconductor

The two-dimensional generalization of a spin-less fermion system that realizes unpaired Majorana fermions is a $p_x + ip_y$ superconductor.² In a continuum model such a superconductor is described by the Hamiltonian [16]

$$H = \int d\mathbf{r} \left\{ \psi^\dagger \left(-\frac{\nabla^2}{2m} - \mu \right) \psi + \frac{\Delta}{2} [e^{i\varphi} \psi (\partial_x + i\partial_y) \psi + \text{H.c}] \right\}. \quad (5.95)$$

Here, ψ creates a spinless fermion with mass m and φ is the phase of the superconducting order parameter $\Delta \in \mathbb{R}$. We consider a system with periodic boundary conditions in both x - and y -directions (a torus). Introducing the notation $\psi_\mathbf{k}^\dagger = [\psi_\mathbf{k}^\dagger, \psi_{-\mathbf{k}}]$ the above Hamiltonian can be written as

$$H = \frac{1}{2} \int \frac{d\mathbf{k}}{(2\pi)^2} \psi_\mathbf{k}^\dagger \mathcal{H}(\mathbf{k}) \psi_\mathbf{k} \quad \text{with} \quad \mathcal{H}(\mathbf{k}) = \sum_i d_i(\mathbf{k}) \sigma_i. \quad (5.96)$$

The d -vector looks like

$$d_x(\mathbf{k}) = -\Delta(k_x \sin(\varphi) + k_y \cos(\varphi)), \quad (5.97)$$

$$d_y(\mathbf{k}) = \Delta(k_x \cos(\varphi) - k_y \sin(\varphi)), \quad (5.98)$$

$$d_z(\mathbf{k}) = \frac{k^2}{2m} - \mu. \quad (5.99)$$

This Hamiltonian is again particle hole symmetric with $U_C = \sigma_x$ as it describes a triplet superconductor. However, due to the $k_x + ik_y$ nature of the pairing, time reversal symmetry is broken,

²So far we have discussed only lattice models. The same can be done for a two-dimensional $p_x + ip_y$ superconductor. However, the main features we want to touch upon are also accessible in a (simpler) continuum model. The interested reader is referred the publication by Asahi and Nagaosa [15] for a lattice version.

which puts us in class D . Hence, we have to calculate the Chern number. The bulk excitation spectrum $\pm d(\mathbf{k})$ is gapped for all values of \mathbf{k} and $\mu \neq 0$. To see if $\mu = 0$ corresponds to a topological phase transition we study the evolution of the d -vector as a function of \mathbf{k} . Remember that we had to regularize the Dirac fermion problem in Sec. 4. One can do so by putting the system on a lattice [15]. Alternatively, we note that for $k \rightarrow \infty$ the director $\hat{d}(\mathbf{k})$ tends to a unique vector which does not depend on the direction of \mathbf{k} . At this point we can cut off the momentum integral as there is no further contribution to the Skyrmiion density $\epsilon_{\alpha\beta\gamma}\hat{d}_\alpha\partial_{k_x}\hat{d}_\beta\partial_{k_y}\hat{d}_\gamma$.³

Let us start with the case $\mu < 0$. Note that for momenta with fixed k , d_x and d_y always sweep out a circle on the unit sphere at height d_z . At $k=0$ we start at the north pole and slowly slide down towards the equator before we move back to the north pole at $k \rightarrow \infty$. Therefore, the d -vector does not wrap around S^2 and the Chern number is zero. For $\mu > 0$ the d -vector starts at the south-pole for $k = 0$ and smoothly moves up to the north-pole at $k \rightarrow \infty$. Hence, the Chern number is non-zero, concretely $C = -1$.

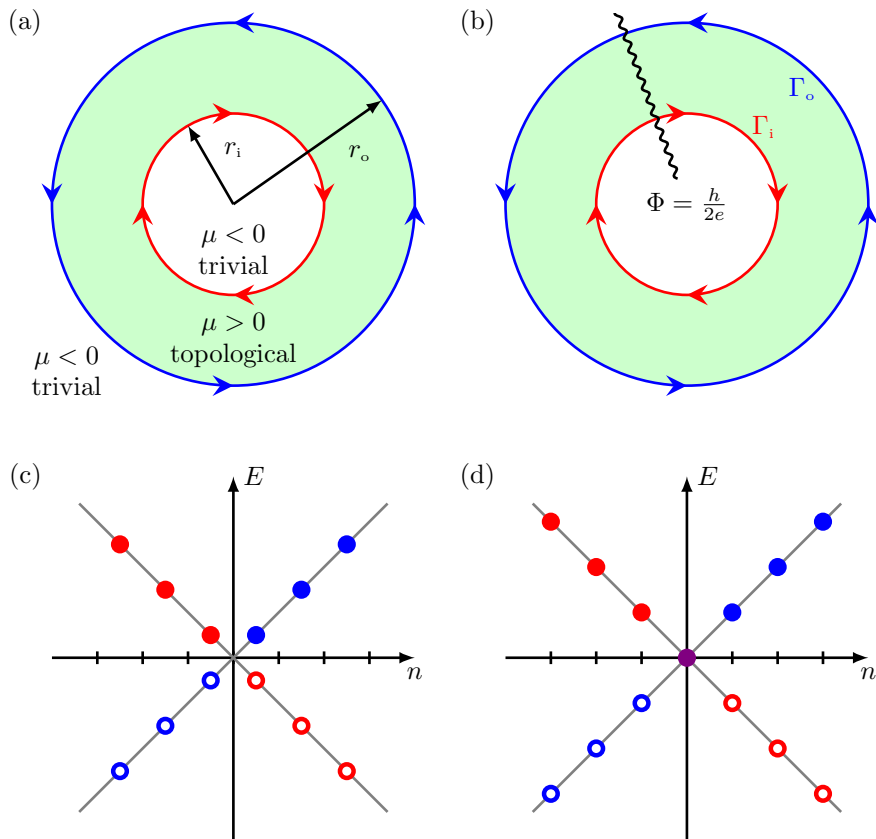


Figure 5.9: (a) Geometry for the chiral Majorana edge modes. (b) Toy model for a vortex in a $p_x + ip_y$ superconductor. (c) Edge spectrum for (a). (d) Spectrum for (b).

As for the Kitaev chain we would like to investigate the physical consequences of this Chern number. We know that at an interface between a topologically trivial and non-trivial region (where the Chern number changes by one) we expect one chiral edge channel. Following the very nice review by Alicea [16], we consider an Corbino disk by assuming the the chemical potential $\mu(r)$ smoothly goes from positive inside the annulus to negative outside, see Fig. 5.9(a). If we are interested in the low-energy modes in the vicinity of the edge and if $\mu(r)$ varies slowly enough,

³This tendency towards a direction independent $\hat{d}(\mathbf{k})$ for large k was not present in the Dirac problem, which resulted in a half-quantized “Chern” number.

we can neglect the ∇^2 -term in the Hamiltonian and write in polar coordinates⁴ (r, ϑ)

$$H_{\text{edge}} = \int d\mathbf{r} \left\{ -\mu(r)\psi^\dagger\psi + \left[\frac{\Delta}{2}e^{i\varphi}e^{i\vartheta}\psi \left(\partial_r + \frac{i\partial_\vartheta}{r} \right) \psi + \text{H.c.} \right] \right\} \quad (5.105)$$

Note that the factor $e^{i\vartheta}$ above means that the pairing couples states with different angular momentum. To simplify this problem with change to new variables⁵

$$\psi \rightarrow \psi' = e^{-i\vartheta/2}\psi. \quad (5.106)$$

It is important to note that in the new variables ψ' , we need to look for solutions with anti-periodic boundary conditions when encircling the annulus. In the new variables $\psi'^\dagger = [\psi'^\dagger, \psi']$ the Hamiltonian is written as $H = \frac{1}{2} \int d\mathbf{r} \psi'^\dagger \mathcal{H}(r, \vartheta) \psi$, with

$$\mathcal{H}(r, \vartheta) = \begin{pmatrix} -\mu(r) & \Delta e^{-i\varphi}(-\partial_r + i\partial_\vartheta/r) \\ \Delta e^{i\varphi}(\partial_r + i\partial_\vartheta/r) & \mu(r) \end{pmatrix}. \quad (5.107)$$

To solve for $\mathcal{H}(r, \vartheta)\chi(r, \vartheta) = E\chi(r, \vartheta)$ we make the Ansatz

$$\chi(r, \vartheta) = e^{i(n+1/2)\vartheta} \begin{pmatrix} e^{-\varphi/2}[f(r) + ig(r)] \\ e^{i\varphi/2}[f(r) - ig(r)] \end{pmatrix}, \quad \text{with } n \in \mathbb{Z}. \quad (5.108)$$

The prefactor $e^{i(n+1/2)\vartheta}$ accounts for the anti-periodic boundary conditions. From the eigenvalue equation we obtain

$$[E - (n + 1/2)\Delta/r]g(r) = -i[\mu(r) - \Delta\partial_r]f(r) \quad (5.109)$$

$$[E + (n + 1/2)\Delta/r]f(r) = i[\mu(r) + \Delta\partial_r]g(r) \quad (5.110)$$

If $\chi(\vartheta, r)$ is well localized around the inner (r_i) or the outer (r_o) radius of the Corbino disk, we can replace $1/r \rightarrow 1/r_{i/o}$. Therefore the above equations have a solution for the outer edge with $f(r) \equiv 0$

$$E_o = \frac{(n + 1/2)\Delta}{r_o}, \quad (5.111)$$

$$\chi_o^n(r, \vartheta) = e^{i(n+1/2)\vartheta} e^{\frac{1}{\Delta} \int_{r_o}^r dr' \mu(r')} \begin{pmatrix} ie^{i\varphi/2} \\ -ie^{-i\varphi/2} \end{pmatrix}. \quad (5.112)$$

⁴ We use

$$x = r \cos(\vartheta) \quad r = \sqrt{x^2 + y^2}, \quad (5.100)$$

$$y = r \sin(\vartheta) \quad \cos(\vartheta) = \frac{x}{\sqrt{x^2 + y^2}} \quad \sin(\vartheta) = \frac{y}{\sqrt{x^2 + y^2}}. \quad (5.101)$$

Therefore

$$\frac{\partial}{\partial x} = \frac{\partial \vartheta}{\partial x} \frac{\partial}{\partial \vartheta} + \frac{\partial r}{\partial x} \frac{\partial}{\partial r} = -\frac{\sin(\vartheta)}{r} \frac{\partial}{\partial \vartheta} + \cos(\vartheta) \frac{\partial}{\partial r}, \quad (5.102)$$

$$\frac{\partial}{\partial y} = \frac{\partial \vartheta}{\partial y} \frac{\partial}{\partial \vartheta} + \frac{\partial r}{\partial y} \frac{\partial}{\partial r} = \frac{\cos(\vartheta)}{r} \frac{\partial}{\partial \vartheta} + \sin(\vartheta) \frac{\partial}{\partial r}. \quad (5.103)$$

The pairing term now reads

$$\partial_x + i\partial_y = [\cos(\vartheta) + i\sin(\vartheta)]\partial_r + [-\sin(\vartheta) + i\cos(\vartheta)]\frac{\partial_\vartheta}{r} = e^{i\vartheta} \left[\partial_r + \frac{i\partial_\vartheta}{r} \right]. \quad (5.104)$$

⁵Remember that this is what we usually do to gauge aways a vector potential for the problem of a particle on a ring. Correspondingly, this transformation induces a term $i\partial_\vartheta \rightarrow i\partial_\vartheta + 1/2$. However, this constant terms vanishes in the pairing due to the Pauli principle.

And for the inner edge with $g(r) \equiv 0$

$$E_i = -\frac{(n+1/2)\Delta}{r_i}, \quad (5.113)$$

$$\chi_i^n(r, \vartheta) = e^{i(n+1/2)\vartheta} e^{-\frac{1}{\Delta} \int_{r_i}^r dr' \mu(r')} \begin{pmatrix} e^{i\varphi/2} \\ e^{-i\varphi/2} \end{pmatrix}. \quad (5.114)$$

These solutions have a few remarkable features. First, there is always a finite energy gap of $\frac{\Delta}{2r_{i/o}}$, see Fig. 5.9. Second, the excitations are chiral with opposite chirality on the inner and outer edge. This looks a bit like the quantum Hall effect. However, here, the edge excitations are not regular complex fermions but are chiral Majorana modes. To see this we consider

$$\psi'(r, \vartheta) = \sum_n [\chi_i^n(r, \vartheta) \Gamma_{in}^n + \chi_o^n(r, \vartheta) \Gamma_{oout}^n]. \quad (5.115)$$

Since the upper and lower components of $\psi'(r, \vartheta)$ are related by Hermitian conjugation, the above equations imply that

$$\Gamma_{i/o}^n = [\Gamma_{i/o}^{-n}]^\dagger. \quad (5.116)$$

This means that the operators

$$\Gamma_{i/o}(\vartheta) = \sum_n e^{in\vartheta} \Gamma_{i/o}^n = \Gamma_{i/o}^\dagger(\vartheta). \quad (5.117)$$

are actually Majorana fermions.

In order to complete this section we show that vortices in a $p_x + ip_y$ superconductor carry a Majorana zero mode. The simplest model for a vortex is to take the annulus of before and thread a flux $h/2e$ through the inner hole. Such a flux quantum gives rise to a phase winding of the order parameter Δ , i.e., $\Delta \rightarrow \Delta(\vartheta) = e^{-i\vartheta} \Delta$. We immediately observe that this swallows the $e^{i\vartheta}$ in (5.105). This in turn, allows us to write the same solutions for ψ instead of ψ' , which obey periodic instead of anti-periodic boundary conditions. Consequently, we have to shift the pre-factor $e^{i(n+1/2)\vartheta} \rightarrow e^{in\vartheta}$ in $\chi(r, \vartheta)$. Hence the energies for the states on the inner edge read now, cf. Fig. 5.9

$$E_{i/o} = \frac{n\Delta}{r_{i/o}} \quad \text{with} \quad n \in \mathbb{Z}. \quad (5.118)$$

In particular the $n = 0$ solution is a zero energy Majorana mode.⁶ To understand the implications of this zero energy Majorana mode we refer to the seminal paper by Ivanov [17].

References

1. Kane, C. L. & Mele, E. J. “Quantum Spin Hall Effect in Graphene”. *Phys. Rev. Lett.* **95**, 226801 (2005).
2. Bernevig, B. A. & Hughes, T. L. *Topological insulators and superconductors* (Princeton University Press, 2013).
3. Haldane, F. D. M. “Model for a Quantum Hall Effect without Landau Levels”. *Phys. Rev. Lett.* **61**, 2015 (1988).
4. Sheng, D. N., Weng, Z. Y., Scheng, L. & Haldane, F. D. M. “Quantum Spin-Hall Effect and Topologically Invariant Chern Numbers”. *Phys. Rev. Lett.* **97**, 036808 (2006).
5. Kohn, W. “Analytic properties of bloch waves and wannier functions”. *Phys. Rev.* **115**, 809 (1959).

⁶ The Majorana property follows from $-n = n$ for $n = 0$, in Eq. (5.116)

6. Nakahara, M. *Geometry, Topology and Physics* (Taylor and Francis, New York and London, 2003).
7. Bohm, A., Mostafazadeh, A., Koizumi, H., Niu, Q. & Zwanziger, J. *The Geometric Phase in Quantum Systems* (Springer-Verlag, Heidelberg, 2003).
8. Kitaev, A. “Periodic table for topological insulators and superconductors”. *AIP Conf. Proc.* **1134**, 22 (2009).
9. Ryu, S., Schnyder, A. P., Furusaki, A. & Ludwig, A. W. W. “Topological insulators and superconductors: tenfold way and dimensional hierarchy”. *New J. Phys.* **12**, 065010 (2010).
10. Schnyder, A. P., Ryu, S., Furusaki, A. & Ludwig, A. W. W. “Classification of topological insulators and superconductors in three spatial dimensions”. *Phys. Rev. B* **78**, 195125 (2008).
11. Qi, X.-L., Hughes, T. L. & Zhang, S.-C. “Topological field theory of time-reversal invariant insulators”. *Phys. Rev. B* **78**, 195424 (2008).
12. Su, W. P., Schrieffer, J. R. & Heeger, A. J. “Solitons in Polyacetylene”. *Phys. Rev. Lett.* **42**, 1698 (1979).
13. Creutz, M. “End States, Ladder Compounds, and Domain-Wall Fermions”. *Phys. Rev. Lett.* **83**, 2636 (1999).
14. Kohn, W. “Construction of Wannier Functions and Applications to Energy Bands”. *Phys. Rev. B* **7**, 4388 (1973).
15. Asahi, D. & Nagaosa, N. “Topological indices, defects, and Majorana fermions in chiral superconductors”. *Phys. Rev. B* **86**, 100504(R) (2012).
16. Alicea, J. “New directions in the pursuit of Majorana fermions in solid state systems”. *Rep. Prog. Phys.* **75**, 076501 (2012).
17. Ivanov, D. A. “Non-Abelian Statistics of Half-Quantum Vortices in p-Wave Superconductors”. *Phys. Rev. Lett.* **86**, 268 (2001).